Clinical, Cosmetic and Investigational Dermatology

Dovepress

Open Access Full Text Article

ORIGINAL RESEARCH

A Retrospective Pragmatic Longitudinal Case-Series Clinical Study to Evaluate the Clinical Outcome of Triple-Frequency Ultrasound in Treatment of Cellulite

Irina Chervinskaya[1], Nadezhda I Kuprina[2], Ilja Kruglikov[3]

[1]Clinic DK Forma, St. Petersburg, Russian Federation; [2]North-West Public Health Research Center, St. Petersburg, Russian Federation; [3]Wellcomet GmbH, Bruchsal, Germany

Correspondence: Ilja Kruglikov, Email i.kruglikov@wellcomet.de

Objective: In this single-centre, retrospective, pragmatic, longitudinal case-series clinical study triple-frequency LDM (TF-LDM) technology with frequencies of 1/3/10 MHz and 3/10/19 MHz was applied for treatment of cellulite to reveal the effect of these waves on the cellulite skin and assess the sustainability of treatment outcomes during the long-term follow-up controls.

Methods: Twenty Caucasian females with mild-to-severe gynoid lipodystrophy aged 27–53 years who received cellulite monotherapy with TF-LDM were included in this study. All participants were evaluated at three time points: baseline (T1), on the day of the last treatment (T2), and during the last follow-up (T3). Cellulite severity was assessed by six independent clinicians using the five-grade Clinician-Reported Photonumeric Cellulite Severity Scale (CR-PCSS). Patient satisfaction was evaluated using a 10-grade GAIS scale, ranging from 0 to 10 (0 - dissatisfied; 10 - fully satisfied). To objectify the treatment outcomes, 17 subjects were investigated using B-mode ultrasonography and real-time compression elastography at baseline and during follow-up.

Results: The average values of CR-PCSS (T1), CR-PCSS (T2) and CR-PCSS (T3) over all participants were 2.22±0.82, 1.18±0.77, and 0.84±0.77, respectively, which corresponded to the skin improvement between T1 and T2 of 0.93±0.27 ($p < 0.0001$) as well as between T1 and T3 of 1.38±0.47 ($p < 0.0001$). Assessment of elasticity of the dermis and adipose tissue on the basis of the 5-grade coloration scale revealed significant reinforcement of both tissues as well as of the superficial fascia at follow-up as compared to their baseline values. The obtained treatment outcomes were long-lasting and could be clearly observed even in individuals with a long-term follow-ups. Assessment of the satisfaction of participants with the treatment results revealed a high satisfaction of 8.95 ± 1.49. The method demonstrated no side effects, was pain-free, well-tolerated, and highly accepted by patients.

Keywords: single-centre, retrospective clinical study, cellulite, triple-frequency ultrasound

Introduction

Cellulite, also known as gynoid lipodystrophy, is a dimpled lumpy skin appearance in the gluteofemoral body area, affecting more than 85% of females over the age of 20 years, whose onset can be seen as early as during puberty. This skin condition is not just an aesthetic problem, but is also associated with the development of negative psychosocial effects in affected individuals. Despite numerous efforts over the last few decades, there are still no effective treatment methods for cellulite with long-lasting treatment outcomes, which may be explained by the lack of a fully understood pathophysiology of this skin condition.

Recently, we have proposed a new pathophysiology of cellulite that explains the most prominent features of this condition including protrusions of the superficial adipose tissue into the dermis, reduced expression of the extracellular glycoprotein fibulin-3, an unusually high presence of the multi-lineage-differentiating stress-enduring (MUSE) cells in gluteofemoral white adipose tissue (gfWAT) as well as a strong spatial association and paracrine interaction of mature adipocytes with sweat glands that is a unique feature of adenolipoma.[1] We have connected these features with selective

Received: 15 October 2024
Accepted: 26 November 2024
Published: 6 December 2024

accumulation of endogenous lipopolysaccharides (LPS, endotoxin) in gfWAT leading to development of a low-grade inflammation in this fat depot. Very recently, we argued that cellulite and lipedema represent consecutive stages of the same process: cellulite represents an early stage and has a high prevalence, whereas lipoedema, with its much lower prevalence, represents the progressive stages of chronic gfWAT modification.[2]

Based on this pathophysiology, the main weak link in cellulite appears to be the layer of skin-associated adipose tissue (SAAT)[3] also known as skin-associated fat (SAF),[4] which is a superficial layer of subcutaneous white adipose tissue (sWAT) adjusted to the reticular dermis. This layer is the human analog of the murine dermal white adipose tissue (dWAT)[5] that attracted much attention during the recent past because of the ability of dermal adipocytes to quickly re- and de-differentiate during the hair follicle cycle[3,6] and to produce the anti-microbial peptide cathelicidin during reactive adipogenesis[7] as well as because of the role of these cells in wound healing and scarring.[3] SAAT in the thighs is located above the superficial fascia and is distinct in its anatomical structure and metabolic properties from the underlying deeper sWAT layer located between the superficial and deep fascia.[8] SAAT has a pronounced lobular structure and highly developed fibrous septa producing the polygonal-oval lobules of mature adipocytes typical in cellulite and connecting dermis with superficial fascia, while the underlying sWAT layer is characterized by smaller, less well-defined and flat lobules as well as by a loose fibrous septa connected to the deep fascia.[1]

SAAT layer demonstrates a high inter-individual variations and a sexual dimorphism being about 1.6 times thicker in females than in males.[4] SAAT and sWAT thicknesses were reported to be 8.41±1.61 mm / 24.81±4.90 mm and 4.03 ±1.26 mm / 4.31±1.82 mm in females with and without cellulite, respectively.[9] As we stated earlier, such significant expansion of SAAT and sWAT layers can sufficiently modify the mechanical behavior of the composite skin/WAT making it more susceptible to mechanical deformations since structural stability of such multi-layered composites strongly depends on the thickness ratios between the neighboring layers, their bending and tensile stiffness as well as adhesive strength between the layers.[10] Stiffness of SAAT and sWAT is much lower than stiffness of stratum corneum or reticular dermis. The expansion of these two thick but mechanically weak adipose layers connected to the weak superficial and deep fascia (this weakness is mainly caused by reduced expression of fibulin-3 in cellulite) significantly modifies the mechanical stability of the dermal-hypodermal interface, allowing protrusions of the SAAT into the dermis.[10] Indeed, interpenetration of neighboring layers is a well-known phenomenon in bi-modular substrates with a tension-compression asymmetry, that is, very different tensile and compressive mechanical moduli.[11] This is generally the case in tissues containing dense collagen networks, where the Young's modulus can be an order of magnitude lower under compression than under extension,[12] and explains the appearance of protrusions on the dermal-hypodermal interface connecting the collagen-rich dermis with the collagen-poor SAAT layer.[1,10] This phenomenon is responsible for the main hallmark of cellulite - distinct protrusions of the underlying adipose tissue into the dermis,[1,13] which significantly affects the architecture of the dermal-hypodermal interface and correlates with cellulite severity.[14]

To make the skin/WAT composite more mechanically stable, and thus improve the visual appearance of cellulite, the superficial layers of this composite (epidermis, dermis, dermal-hypodermal interface, and SAAT) must be sufficiently reinforced. Reinforcement of the epidermis and reticular dermis is needed to reduce the projections of WAT protrusions to the skin surface, whereas reinforcement of the SAAT and superficial fascia is necessary to adjust the stiffness of the reticular dermis to the stiffness of the SAAT, thus reducing the protrusions on the dermal-hypodermal interface. As we demonstrated earlier, the production of collagen in dermal adipocytes exceeds its production in their subcutaneous counterparts by several times,[3] which allows a selective reinforcement of the dermal-hypodermal interface. Of note, protrusions of SATA into the dermis are also significantly increased in aged skin and can serve as a hallmark of skin aging,[15] which indirectly supports the earlier assumption that cellulite is associated with premature skin aging in the gluteofemoral area.[16]

Selective reinforcement of the skin/WAT composite can be achieved through activation of transforming growth factor beta (TGF-β), which is a master regulator of collagen production and fibrosis.[17] TGF-β signaling is tightly connected with plasma membrane structures known as caveolae, which are plasma membrane invaginations that are highly abundant in mechanically stressed cells and play an important role in cellular signaling. Stability of caveolae is mainly regulated by caveolin-1 (CAV1), which vigorously interacts with TGF-β membrane receptors and can be internalized through CAV1-dependent endocytosis.[17,18] CAV1 is also strongly linked to the actin cytoskeleton, and modification of this intracellular network sufficiently affects the content of CAV1 in the plasma membrane. This modification can be provided, among others, by application of the high-frequency ultrasound waves, whereas higher ultrasound frequencies and intensities cause a stronger fluidization of the cytoskeleton structure.[17,19] This effect can be further enhanced by a quasi-simultaneous application of different ultrasound waves, known as the local dynamic micro-massage (LDM) technology.[20] These properties of the high-frequency LDM waves warrant their application for aesthetic indications such as cellulite and skin tightening.

The main problem with existing treatment options for cellulite is the low sustainability of treatment outcomes, which usually disappear relatively quickly after the cessation of treatment.[21] This demands regular maintenance treatments and substantially reduces the acceptance of existing anti-cellulite treatment methods by patients. In this retrospective longitudinal case-series study, we applied triple-frequency LDM (TF-LDM) waves with frequencies of 1/3/10 MHz or 3/10/19 MHz for the treatment of cellulite to reveal the effect of these waves on cellulite skin and assess the sustainability of treatment outcomes using photonumeric assessment and sonoelastography during long-term follow-up controls.

Methods

Participants

Twenty Caucasian females with mild-to-severe gynoid lipodystrophy aged 27–53 years who received the monotherapy of cellulite with TF-LDM were included in this study (Table 1). Participants # 2 and #19 demonstrated a high laxity of the

Table 1 Subjects and Their Treatment Parameters

Subject	Age, year	Sessions	Follow-up, Months
1	34	8	8.5
2	53	8	18.0
3	41	10	17.0
4	39	10	17.0
5	28	10	11.0
6	46	10	6.5
7	36	10	9.5
8	37	10	10.5
9	33	10	10.0
10	47	10	3.0
11	48	10	4.5
12	52	10	6.0
13	48	10	6.5
14	39	10	5.5
15	52	10	6.0
16	40	8	10.0
17	35	10	4.0
18	36	10	4.5
19	45	10	5.0
20	27	10	4.0

skin at baseline and were diagnosed with undifferentiated connective tissue dysplasia (UCTD). Individuals who did not finish the treatment course, individuals with advanced-stage lipoedema, and individuals who received cellulite treatment with any other treatment methods during the last year were excluded from this study. Written informed consent was obtained from all patients.

Study Design

This was a single-centre, retrospective, pragmatic, longitudinal case-series clinical study. Because the participants could clearly identify the treatment with ultrasound waves,[22] neither the participants nor the study nurses or doctors were blinded. The study was conducted with a LDM Triple device operating with TF-LDM waves of 1/3/10 MHz and 3/10/19 MHz (Wellcomet GmbH, Germany). In the LDM technology, the single ultrasound frequencies alternate quickly (every 1–10 ms) (Figure 1). Because neither the cells nor the tissues can develop a full reaction to a single mechanical impact of several milliseconds, they are forced to react simultaneously to all applied frequencies, producing the effect that was named "biological interference".

The treatments were provided at the DK Forma Clinic (St. Petersburg, Russia). All individuals were treated 1–2 times per week for 8–10 sessions (Table 1). As demonstrated in a preliminary pilot study conducted with LDM Triple device by Dr. Kim Sojung (Llas Clinic, Seoul, Korea), this number of sessions was sufficient to provide stable improvement in cellulite appearance (personal communication). During the treatment, the whole affected gluteofemoral area and the thighs were treated uniformly with a standard program "Cellulite" operating with the following treatment parameters: 1/3 MHz (1.5/1.5 W/cm^2, 6 min), 1/3/10 MHz (1.5/1.5/1.5 W/cm^2, 6 min) on each side of the body, which made this study to a pragmatic one. All participants received several follow-up controls, with the last follow-up ranging from 3 months to 18 months after the last treatment (Table 1). Additionally, three individuals (#11-13) were treated contra-laterally with TF-LDM waves of 1/3/10 MHz and 3/10/19 MHz to compare the effects of TF-LDM waves with different penetration depths and thus different energy distributions in the composite skin/WAT. The sides of the TF-LDM application in these three patients were randomized. A standard ultrasound gel without any additional pharmacological drugs was used as the coupling medium.

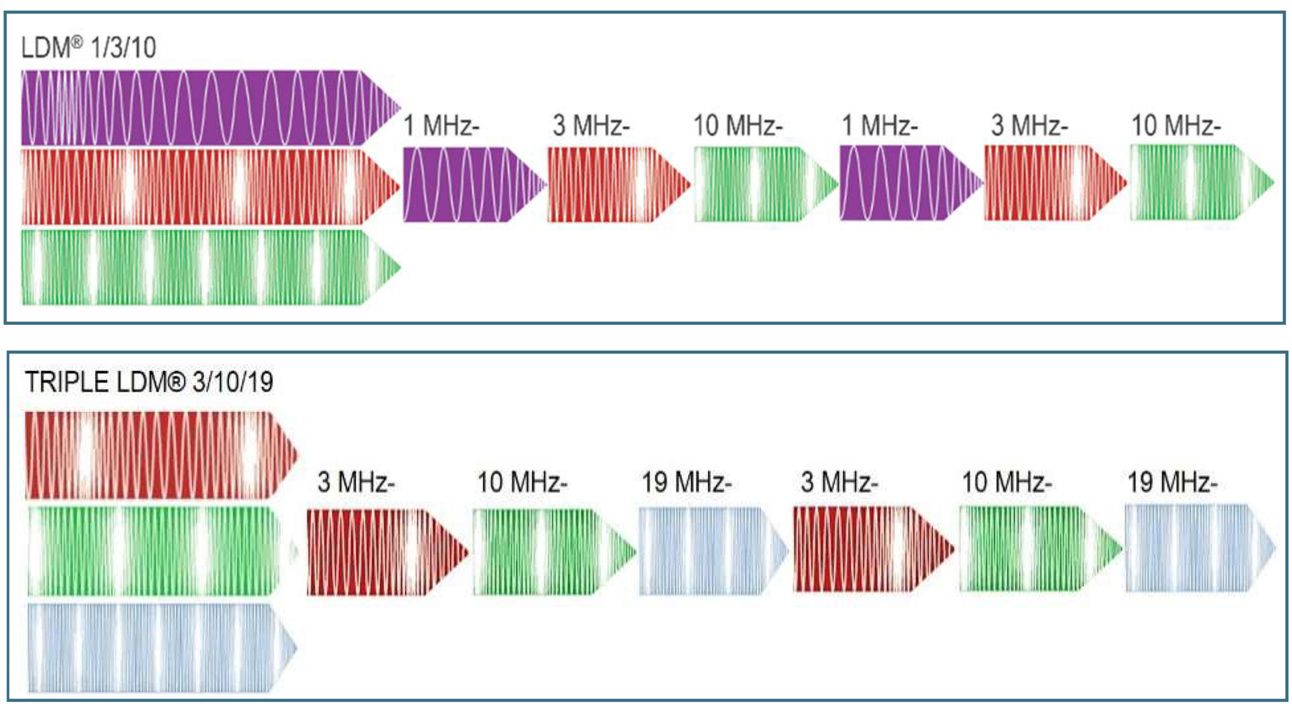

Figure 1 Wave formation in triple-frequency LDM modus: (**top**) – 1/3/10 MHz, (**bottom**) - 3/10/19 MHz.

Clinical Assessment

All participants who completed the treatment course were evaluated at three time points: baseline (T1), on the day of the last treatment (T2), and during the last follow-up (T3). Intermediate follow-up controls were documented, but not evaluated in this study. Cellulite severity was assessed by six independent clinicians using the five-grade Clinician-Reported Photonumeric Cellulite Severity Scale (CR-PCSS) (0 - none, 1 - almost none, 2 - mild, 3 - moderate, 4 - severe) developed and validated to evaluate cellulite severity in the gluteofemoral area.[23,24] Pre- and post-treatment photographs of the affected gluteofemoral areas were taken in a special room to avoid the influence of outside light conditions. Patient satisfaction was evaluated using a 10-grade GAIS scale, ranging from 0 to 10 (0 - dissatisfied; 10 - fully satisfied).

To objectify the treatment outcomes, 17 participants underwent B-mode ultrasonography at baseline and during follow-up using an ultrasound scanner model HS50 (Samsung Medison, Republic of Korea). The modification of soft tissue caused by the application of TF-LDM waves was investigated using real-time compression elastography, which allows simultaneous display of B-mode images and sonoelastograms. Tissue stiffness was visualized using the ElastoScan™ technique (linear array probe LA3-16A operating with frequencies of 3.0–16.0 MHz) based on the strain elastography method, which allows the conversion of the strains induced in the soft tissue by ultrasound waves into colour images (red - very low, yellow - low, green - intermediate, blue - high stiffness). Elasticity of the dermis and adipose tissue was assessed using a 5-grade scale: 1 - predominantly red, 2 - mixed yellow/red, 3 - mixed green/yellow, 4 - mixed blue/green, and 5 - predominantly blue. Assessment was performed for six areas (gluteal left/right, femoral left/right, and lateral left/right) at baseline and follow-up. The corresponding areas are displayed in the upper-right corner of the sonoelastographic images. Ultrasonographic and sonoelastographic investigations were performed by the North-West Public Health Research Center (St. Petersburg, Russian Federation), which explains why the follow-up terms for sonoelastography deviated from the follow-up terms for the photonumeric assessment in the same patients.

Statistical Analysis

Statistical analysis was performed using statistic software RStudio (Posit PBC, Boston, USA) ver. 2023.09.1+494 (IBM), by Easy Statistik (Aachen, Germany). Data were calculated for each participant and for the whole cohort at all three time points T1-T3 and expressed as the mean ± standard deviation. To increase the probability of recognition of the small effects, especially between the time points T2 and T3, we have applied the cohort analysis, which considers all assessments for all patients and allows to significantly increase the sample size and correspondingly the statistical power. Since preliminary assessment of the distribution of the CR-PCSS scores using the Shapiro–Wilk test demonstrated a non-normal distribution of variables, the non-parametric Wilcoxon signed-rank test with continuity correction was applied to compare the CR-PCSS scores at baseline and after the TF-LDM treatment course as well as during the last follow-up control for the single participants and for the whole cohort. Quantile-quantile plots were used to assess the distribution of CR-PCSS data at each time point T1-T3. The same Wilcoxon test was applied to compare the elastic scores of the dermis and SAAT at baseline and during follow-up. The Bayesian *t*-test was applied to verify the statistical significance of the data obtained using the Wilcoxon test for elastic scoring. Differences were considered statistically significant at $p < 0.05$.

Results

Photonumeric Assessment

The descriptions of the patients, their treatments, and follow-up data are presented in Table 1. In this study, the age of the participants was 27–53 (40.80 ± 7.58) years. They received 8–10 (9.6 ± 1.0) treatments with TF-LDM and had the multiple follow-up controls with the last follow-up ranging between 3 and 18 (8.35 ± 4.44) months after the last treatment (Table 1).

The CR-PCSS assessments provided by six clinicians at time points T1-T3 are presented in Table 2. The average values of CR-PCSS (T1), CR-PCSS (T2) and CR-PCSS (T3) for the total cohort of participants were 2.22±0.82, 1.18±0.77, and 0.84±0.77, respectively. This corresponds to the skin improvement of 0.93±0.27 between T1 and T2, of 1.38±0.47 between T1 and T3, and of 0.33±0.38 between T2 and T3. These results are shown in Figure 2.

Table 2 Assessment of the Cellulite Severity at Baseline (T1), on the Day of the Last Treatment (T2) and During the Last Follow-Up Control (T3)

Patient	CR-PCSS (T1)	CR-PCSS (T2)	CR-PCSS (T3)
1	2.17±0.75	1.17±0.75	0.83±0.41
2	2.00±0.00	1.00±0.00	1.67±0.52
3	2.50±0.55	0.50±0.55	0.17±0.41
4	1.50±0.55	1.00±0.00	0.33±0.82
5	2.50±0.55	1.17±0.41	1.00±0.00
6	3.33±0.52	2.17±0.41	1.00±0.00
7	1.00±0.00	0.33±0.52	0.00±0.00
8	2.00±0.00	1.00±0.00	0.83±0.41
9	1.33±0.52	0.33±0.52	0.00±0.00
10	2.33±0.52	1.33±0.52	1.00±0.00
11	3.17±0.41	2.00±0.00	1.00±0.00
12	4.00±0.00	3.00±0.00	3.00±0.00
13	3.33±0.52	2.33±0.52	2.00±0.00
14	2.17±0.41	1.17±0.41	0.83±0.41
15	2.33±0.52	1.33±0.52	0.50±0.55
16	1.00±0.00	0.00±0.00	0.00±0.00
17	2.00±0.00	1.00±0.00	1.00±0.00
18	1.50±0.55	0.50±0.55	0.00±0.00
19	2.83±0.41	1.83±0.75	1.50±0.55
20	1.33±0.52	0.33±0.52	0.17±0.41

Patients #2 and #19, who were diagnosed with UCTD, had slower improvement than other participants. Patient #2 was the only participant who demonstrated a decrease in treatment outcome in a late follow-up of 18 months (1.67±0.52) compared to the outcome observed on the day of the last treatment (1.00±0.00).

Ultrasonographic Investigation

The application of real-time compression sonoelastography allows the simultaneous display of B-mode images and sonoelastograms (Figure 3). Ultrasonographic investigation of cellulite skin in B-mode revealed that the dermal-hypodermal interface in untreated patients with cellulite has an irregular structure. The superficial fascia demarcating the boundary between the SAAT and the sWAT appeared at baseline as a thin hyperechogenic layer. After 8–10 treatments with TF-LDM, the dermal-hypodermal interface was reinforced and appeared as a regular structure, whereas the superficial fascia appeared thicker than at baseline.

Sonoelastographic visualization of tissue stiffness with ElastoScan^{TM} in intact cellulite skin revealed multiple areas of reduced stiffness in the dermis and SAAT as well as weak structures of the superficial fascia, which were colored yellow and/or red. The stiffness of the dermis and SAAT significantly increased after treatment with TF-LDM waves, as indicated by the appearance of green and blue colours in the corresponding sonoelastographic images. Assessment of

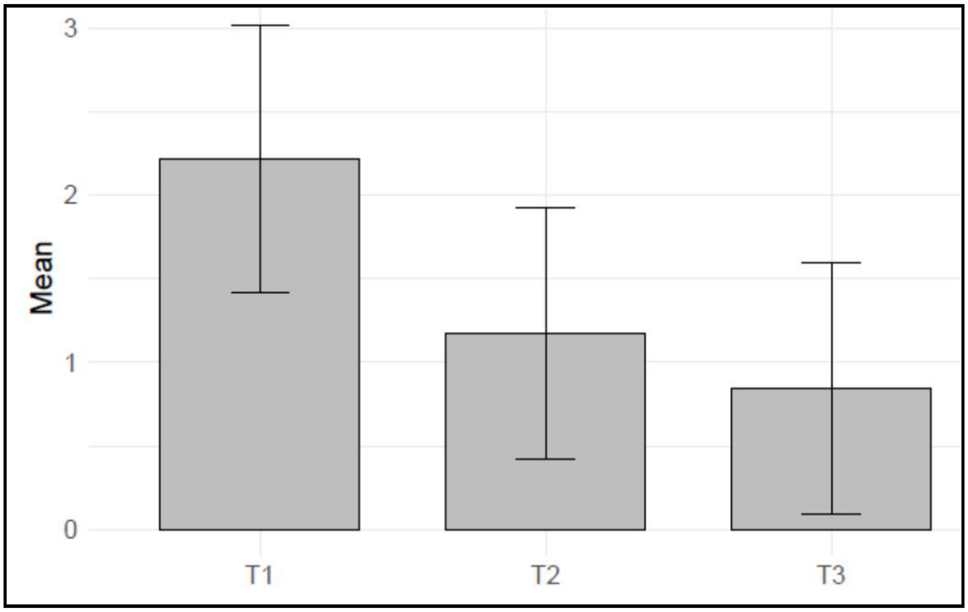

Figure 2 The mean CR-PCSS values were evaluated at the time points T1, T2, and T3. All CR-PCSS differences between the scores at T1 and T2, T2 and T3, and T2 and T3 (calculated for the entire cohort of participants) were highly statistically significant ($p < 0.0001$).

elasticity of the dermis and SAAT using the 5-grade coloration scale revealed significant reinforcement of both tissues as well as of the superficial fascia at follow-up as compared to their baseline values (see Table 3 and Figure 4). The average values for elastic scores before and after treatment with TF-LDM waves were 2.96±0.54 vs 4.08±0.48 (dermis) and 2.91 ±0.65 vs 3.91±0.60 (SAAT). These improvements were statistically significant with $p < 0.001$.

Because of a very high significance of the results for elastic scoring presented in Table 3, we verified them by applying the Bayesian *t*-test. Bayes factors calculated for different areas of the dermis and SAAT (see Table 3) for the paired data at baseline vs follow-up were far above the critical value of 100 that is in the theory considered as "decisive" for the evidence for existing treatment effect, which additionally supported a significant modification of the elasticity in the dermis and SAAT after treatment with TF-LDM waves.

Typical modifications of the cellulite skin and sonoelastographic images before and after application of TF-LDM waves observed in this study are shown in Figures 5 and 6. Figure 5 demonstrates the photographs of patient #11 at baseline, after 10 treatments with TF-LDM at 1/3/10 MHz (left side) and 3/10/19 MHz (right side), and at 4.5 months follow-up for the relaxed and pinched gluteofemoral area. The average CR-PCSS score by this patient was improved from 3.17±0.41 at baseline to 2.00±0.00 after treatment ($p < 0.05$) and further to 1.00±0.00 at 4.5 months follow-up control ($p < 0.05$). Figure 6 presents sonoelastographic images for different parts of the gluteofemoral area of the same patient before and after treatment with TF-LDM waves. It can be clearly seen that TF-LDM treatment significantly increased the stiffness of the soft tissue, which was especially pronounced in the dermis and SAAT. At the same time, application of TF-LDM waves of 3/10/19 MHz (a-d) resulted in a distinctly stronger increase in the stiffness of the dermis and SAAT as compared to the TF-LDM waves of 1/3/10 MHz (e-h).

Examples of the treatment outcomes obtained in this study are shown in Figures 7–11. These results demonstrate a photonumeric improvement in the cellulite skin and an objective increase in the stiffness of the soft tissue in the targeted area after treatment with TF-LDM waves.

Satisfaction of Participants with Treatment Results

Cellulite treatments with TF-LDM waves of both 1/3/10 MHz and 3/10/19 MHz had no side effects, were pain-free, well tolerated, and highly accepted by participants. A majority of the patients reported sufficient improvement in their psychosocial state and self-confidence after treatment. Assessment of the satisfaction of participants with treatment

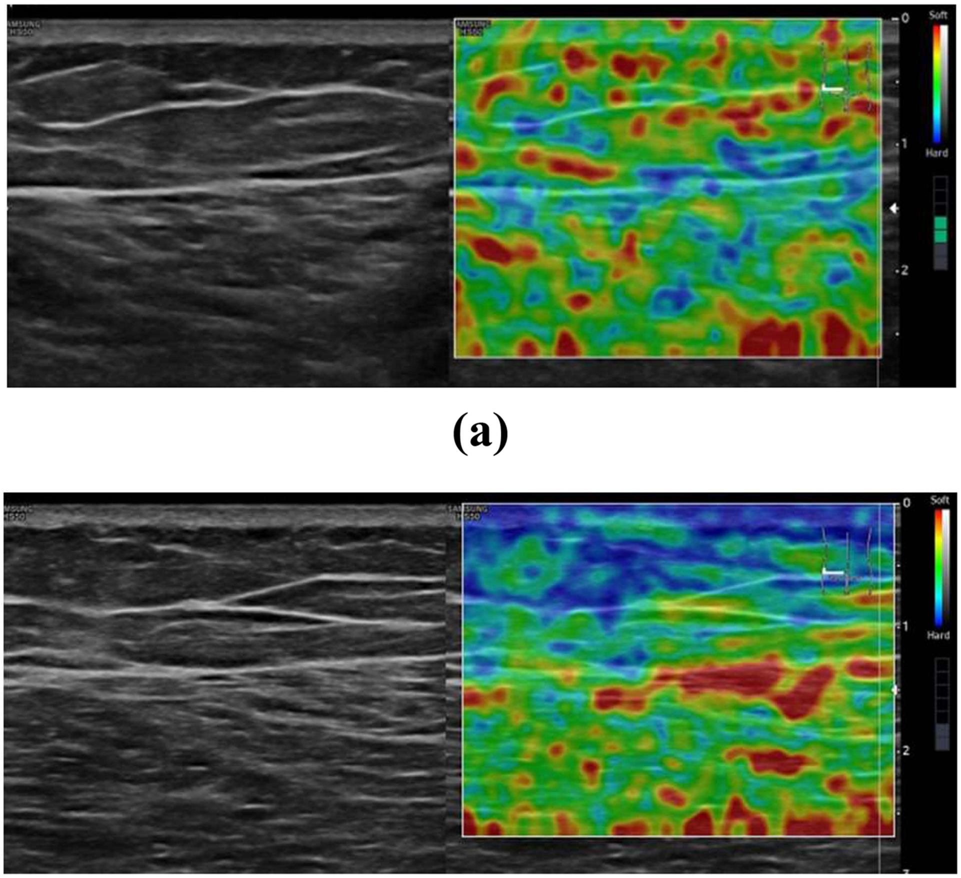

(a)

(b)

Figure 3 B-mode images and elastograms obtained using real-time sonoelastography: (**a**) at baseline and (**b**) at 4.5 months follow-up after 10 TF-LDM. B-mode images demonstrate the changes in echogenicity of the skin and subcutaneous adipose tissue as well as in the structure of superficial and deep fascia. The colour bar on the upper right of the images shows the scale of the relative stiffness of the tissue.

results provided on the basis of a 10-grade GAIS scale between 0 and 10 revealed an average satisfaction of 8.95 ± 1.49 (ranged between 5 and 10), whereas 11 participants scored their satisfaction with 10, three with 9, and three with 8. Three other participants (#14, #18, and #19) assessed their satisfaction with 7, 6, and 5 points, respectively, which highly likely reflects their false expectations. For illustration, Figure 12 shows photographs and sonoelastograms of participant #18 (satisfaction score 6) at baseline and at follow-up control 4.5 months after the last treatment.

Table 3 Elastic Scores (ES) of the Dermis and SAAT at Baseline and During the Follow-Up Sonographic Investigation

Area	ES SAAT at Baseline	ES SAAT at Follow-up	ES dermis at Baseline	ES dermis at Follow-up
Gluteal, left	3.00±0.61	4.00±0.61*	3.06±0.43	4.24±0.56*
Gluteal right	2.94±0.65	3.88±0.60*	3.12±0.33	4.12±0.33*
Lateral, left	2.71±0.59	3.82±0.53*	2.82±0.53	4.00±0.35*
Lateral, right	2.94±0.56	3.82±0.53*	3.00±0.50	4.06±0.56*
Femoral, left	2.82±0.81	4.06±0.56*	2.94±0.75	4.06±0.56*
Femoral, right	3.06±0.66	3.88±0.78*	2.82±0.64	4.00±0.50**

Notes: Statistical differences between baseline and corresponding follow-up: *) $p < 0.001$ and **) $p < 0.002$.

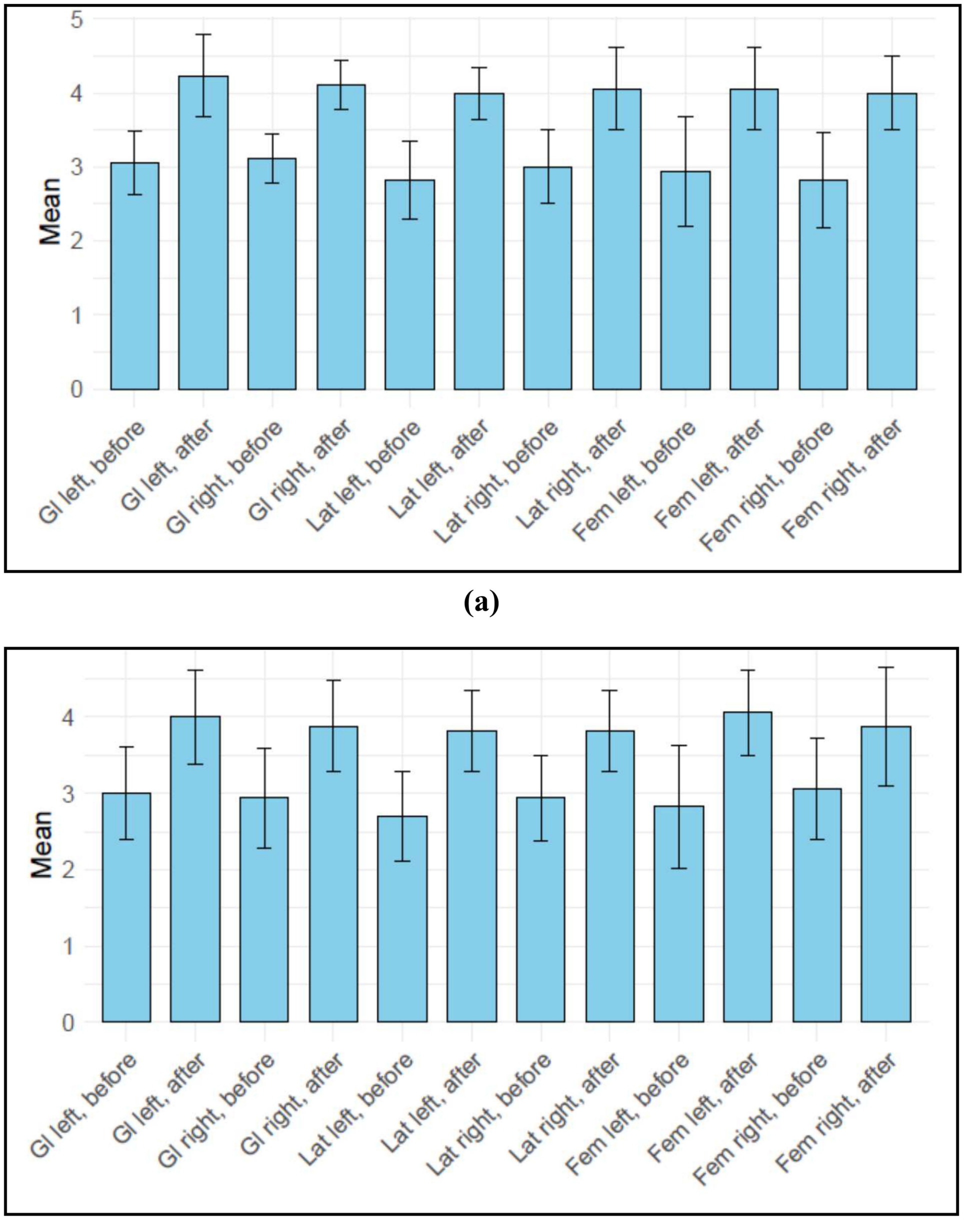

(b)

Figure 4 Elastic scores of the dermis and SAAT for six investigated areas (gluteal, lateral, and femoral) at baseline and follow-up: (**a**) dermis, (**b**) SAAT.

Discussion

As demonstrated in previous studies, LDM waves can be effectively used for treatment of different skin conditions.[20,25,26] The results obtained in the present study demonstrated a significant improvement of the cellulite skin after treatment with TF-LDM with frequencies of 1/3/10 MHz and 3/10/19 MHz. The CR-PCSS scores, as assessed by six independent therapists, improved in all 20 patients. Specifically, there was an improvement of CR-PCSS score of 0.93±0.27 ($p < 0.0001$) between T1 and T2, of 1.38±0.47 ($p < 0.0001$) between T1 and T3, and of 0.33±0.38 ($p < 0.0001$) between T2 and T3. Thus, the average improvement in cellulite skin between the baseline and follow-up controls was more than one grade in accordance with the CR-PCSS scale.

Earlier, the extracellular glycoprotein fibulin-3 (EFEMP1) was reported to be significantly reduced both in cellulite skin and in fibrous septa.[13] Generally, such deficiency of EFEMP1 causes a reduction of elastic fibers leading to the

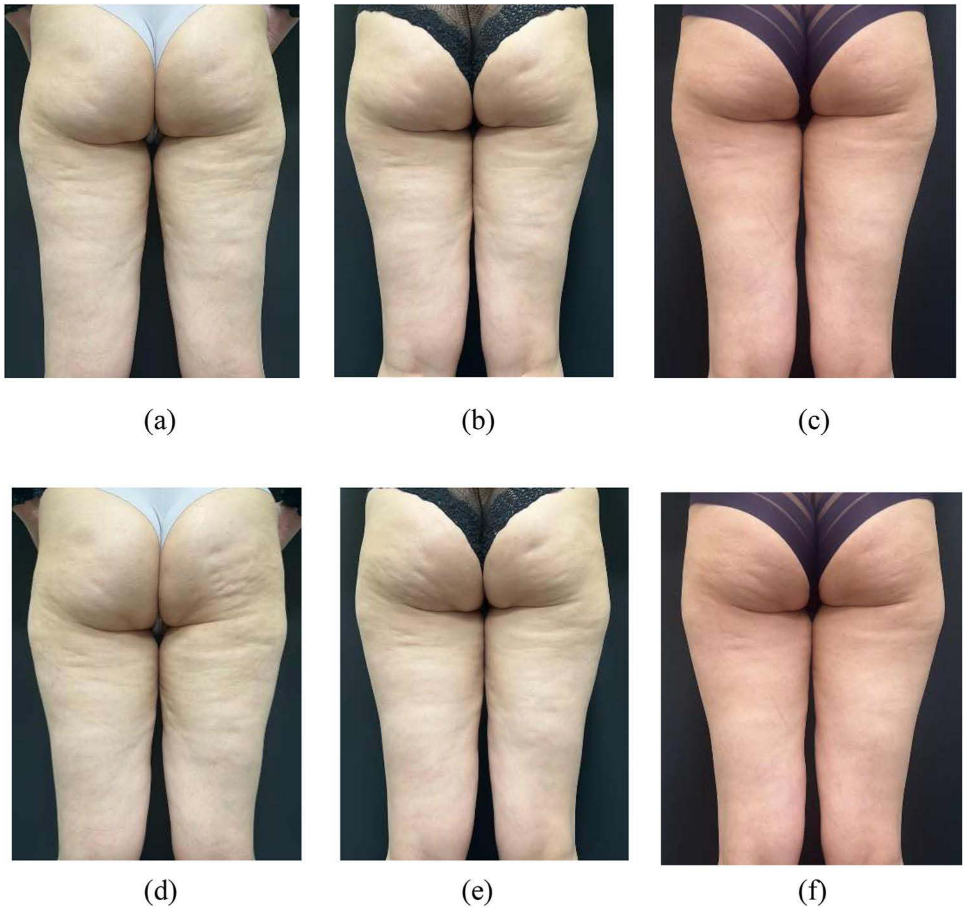

Figure 5 Patient #11: (**a** and **d**) at baseline, (**b** and **e**) after 10 treatments with TF-LDM of 1/3/10 MHz (left side) and 3/10/19 MHz (right side), (**c**) at 4.5 months follow-up; (**a-c**) relaxed, (**d-f**) pinched.

development of weakness of the fascia, tissue herniation and even to prolapse.[27] Mechanical loading up-regulates EFEMP1 expression,[28] thus reversing the morphological modifications caused by EFEMP1 deficiency. In this study, such mechanical loading was provided by application of TF-LDM waves; however, it should be noted that the strains induced by these waves in the soft tissue are frequency dependent.[17] The stiffness of the superficial fascia was improved after treatment with TF-LDM waves, which strongly suggests that TF-LDM waves effectively modulate EFEMP1 expression in the skin and WAT; however, this issue requires additional validation in future research.

Sonoelastography revealed a highly significant increase in the stiffness of the dermis and SAAT after treatment with TF-LDM waves (Table 3) which correlated with improvement in the optical cellulite appearance (see Figures 6, 7 and 9–12). Additionally, objective control provided with ultrasonography in B-mode demonstrated that application of TF-LDM waves sufficiently improved the dermal-hypodermal interface, which was modified from irregular to an even and continuous boundary. This confirms our previous assumption that the main targets in cellulite must be the reinforcement of the epidermis, dermis, SAAT, and dermal-hypodermal interface.[1] Such reinforcement causes a reduction in the protrusions of SAAT into the dermis, thus reducing the internal pressure on the skin surface and simultaneously increasing the resistance of the skin to deformations caused by residual protrusions.

Comparison of the sonoelastograms in participants treated contralateral with TF-LDM waves of 1/3/10 MHz and 3/10/19 MHz demonstrated that the application of TF-LDM at 3/10/19 MHz produced much stronger reinforcement of the upper layers of the skin/WAT composite, especially of the epidermis, dermis, and SAAT (Figure 6). This effect should be connected to both the frequency-dependent absorption of ultrasound waves in the skin and WAT and to a stronger mechanical effect induced by ultrasound waves of higher frequencies. Indeed, ultrasound waves with frequencies of 1 MHz, 3 MHz, 10 MHz, and 19 MHz have the half-value penetration depths in the body of about 30 mm, 10 mm, 3 mm

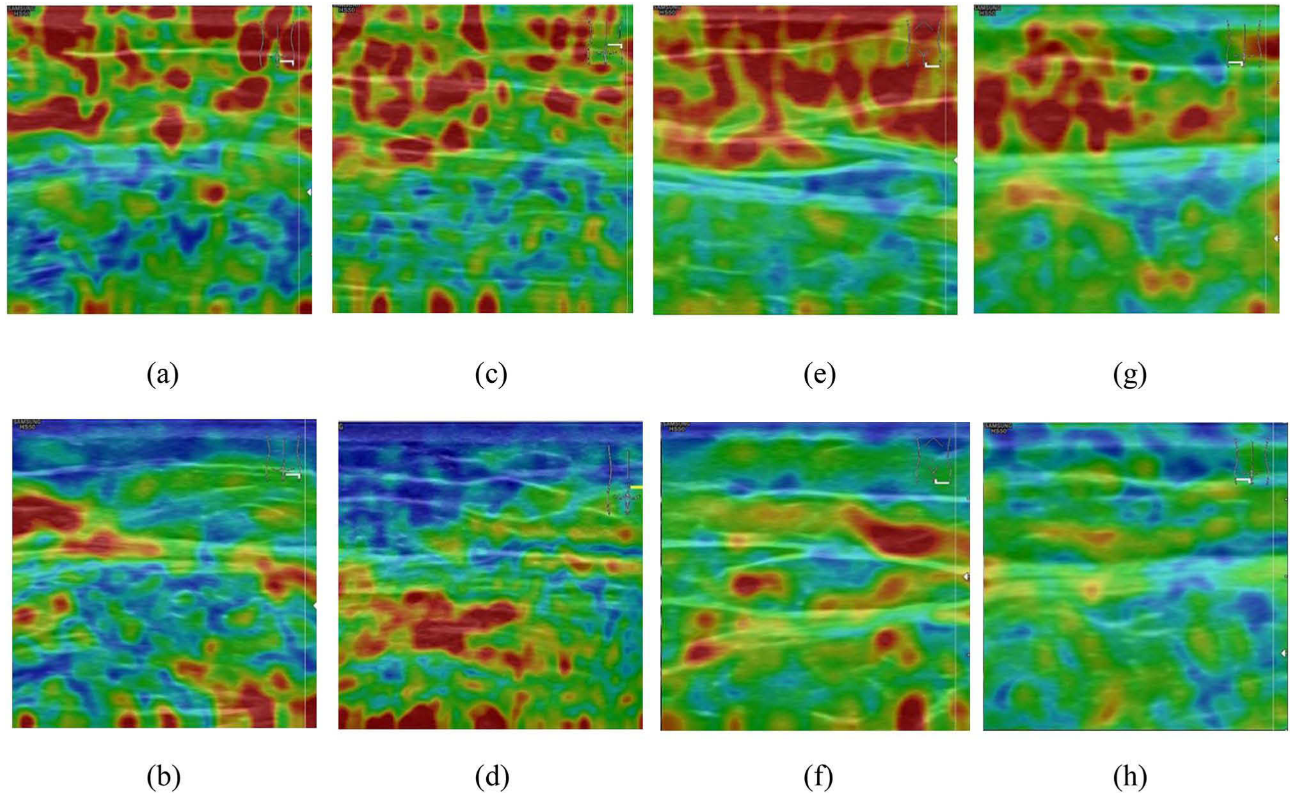

Figure 6 Sonoelastographic images of different parts of the gluteofemoral area (shown in the upper right of the images) of patient #11: (**a, c, e, g**) at baseline; (**b, d, f, h**) 4.5 months follow-up after 10 treatments with TF-LDM of 1/3/10 MHz (left side) and 3/10/19 MHz (right side); (**a** and **b**) and (**c** and **d**) - treatment with TF-LDM of 3/10/19 MHz, (**e** and **f**) and (**g** and **h**) – treatment with TF-LDM of 1/3/10 MHz.

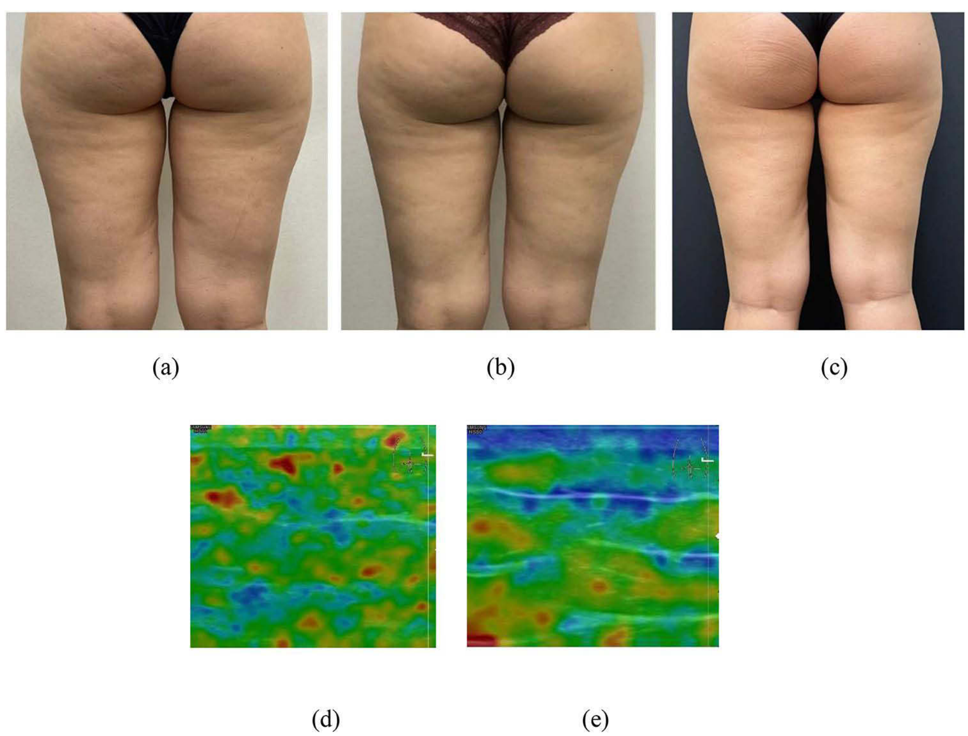

Figure 7 Patient #4: (**a**) at baseline, (**b**) after 10 treatments with TF-LDM of 1/3/10 MHz, (**c**) at 17 months follow-up; (**a–c**) relaxed. Sonoelastography (**d**) at baseline and (**e**) at 5 months follow-up.

(a) (b) (c)

Figure 8 Patient #6: (**a**) at baseline, (**b**) after 10 treatments with TF-LDM of 1/3/10 MHz, (**c**) at 6.5 months follow-up; (**a**–**c**) relaxed.

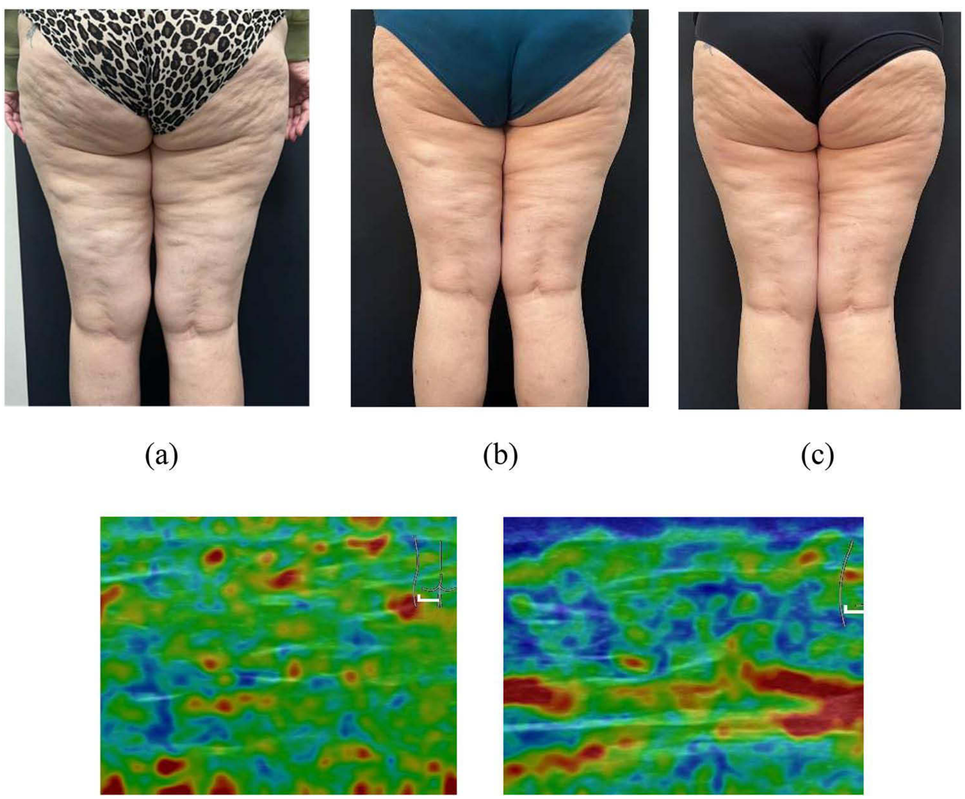

(a) (b) (c)

(d) (e)

Figure 9 Patient #12: Contralateral treatment with TF-LDM of 1/3/10 MHz (left side) and TF-LDM of 3/10/19 MHz (right side): (**a**) at baseline, (**b**) after 10 treatments, (**c**) at 3.5 months follow-up; (**a**–**c**) pinched. Sonoelastography (**d**) at baseline and (**e**) at 2.0 months follow-up.

and 1.5 mm, respectively, which means that application of the TF-LDM waves of 1/3/10 MHz and 3/10/19 MHz allows different in-depth treatment of the cellulite skin.

Structural modifications of the dermis and SAAT provided by TF-LDM waves were remarkably long-lasting. The last follow-up control in participating individuals ranged between 3 to 18 months and was in average 8.35 ± 4.44 months after the last treatment. In these controls, 16 participants demonstrated further improvement, and 3 participants had the same treatment outcomes as on the day of the last treatment. Only participant #2 (who was diagnosed with UCTD) demonstrated a reduction in treatment outcome at 18 months follow-up compared with the cellulite state after the last treatment. This distinguishes this

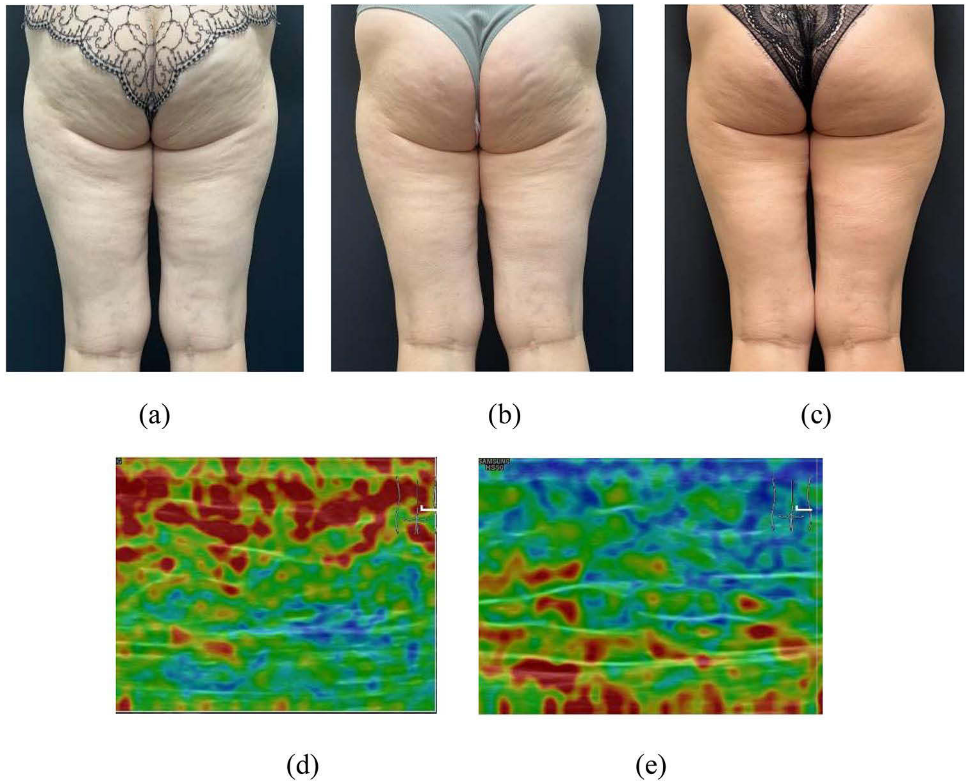

Figure 10 Patient #14: (**a**) at baseline, (**b**) after 10 treatments with TF-LDM of 1/3/10 MHz, (**c**) at 5.5 months follow-up; (**a**–**c**) pinched. Sonoelastography (**d**) at baseline and (**e**) at 5.5 months follow-up.

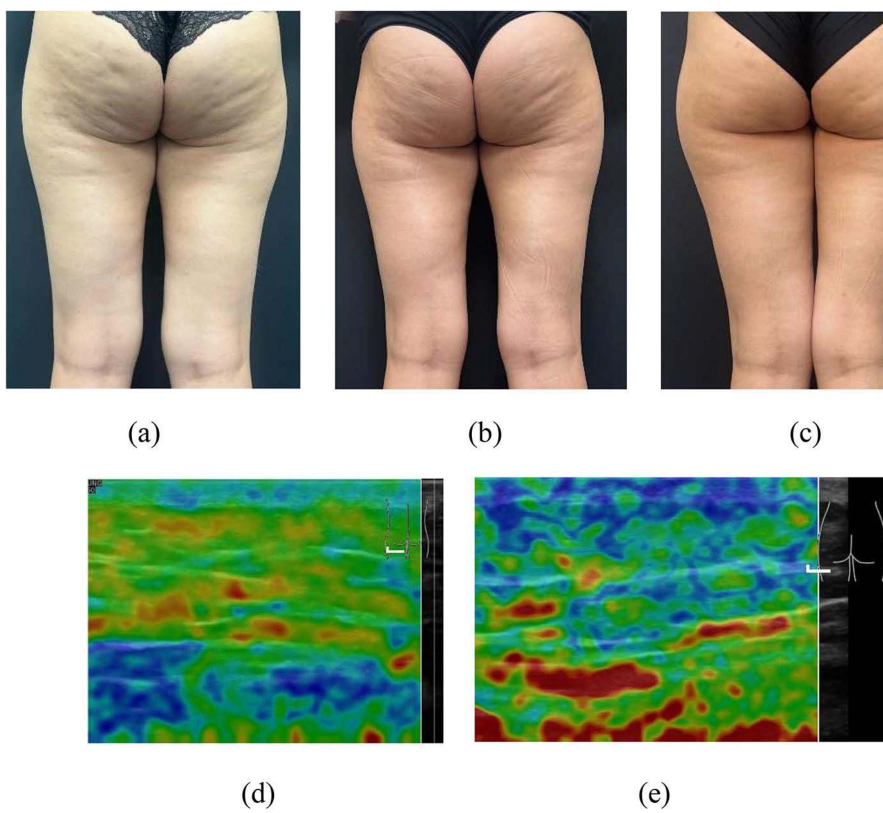

Figure 11 Patient 17: (**a**) at baseline, (**b**) after 10 treatments with TF-LDM of 1/3/10 MHz, (**c**) at 4.0 months follow-up; (**a**–**c**) pinched. Sonoelastography (**d**) at baseline and (**e**) at 3 months follow-up.

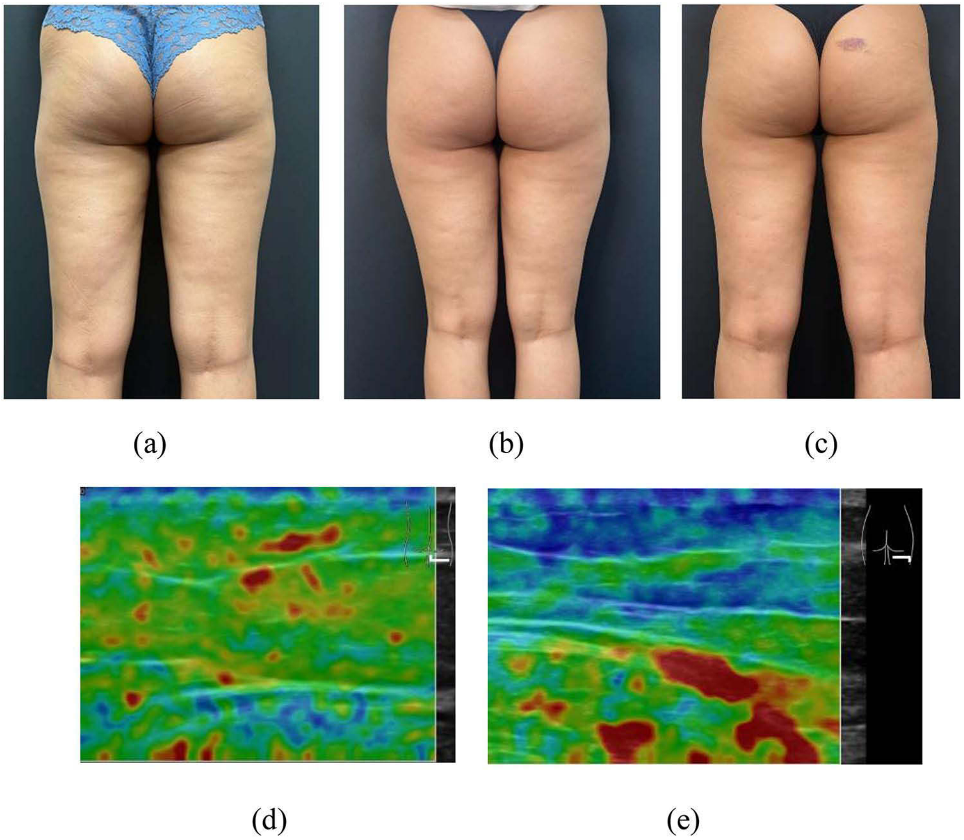

Figure 12 Patient #18: (**a**) at baseline, (**b**) after 10 treatments with TF-LDM of 1/3/10 MHz, (**c**) at 4.5 months follow-up; (**a**–**c**) relaxed. Sonoelastography (**d**) at baseline and (**e**) at 4.0 months follow-up.

method from other cellulite treatment options, which normally demonstrate a decay in treatment outcomes with a relatively short time constant of several months.

Remarkably, we were not able to detect any significant decay in treatment outcomes by participants (except patient #2 with UCTD) even during long-term follow-up controls, which could be mainly explained by a very strong reinforcement of the dermis and SAAT observed sonoelastographically in patients treated with TF-LDM waves (Table 3).

The results obtained in this study demonstrate that the application of TF-LDM waves with higher frequencies of 3/10/19 MHz produces more pronounced treatment outcomes in the dermis and superficial WAT, while the lower frequencies of 1/3/10 MHz produce an additional improvement in the stiffness of subcutaneous WAT, which highlights that the application of both waves can lead to further improvement of treatment outcomes. This topic should be investigated further in future studies. Another open question remains whether an additional treatment course with TF-LDM waves can further improve the state of cellulite.

As we argued earlier, appearance of cellulite should be connected with selective accumulation of endogenous endotoxins in gfWAT leading to production of the low-grade inflammation in this fat depot.[1] This effect is induced by translocation of endotoxins from intestine into circulation caused by decreased barrier function of the intestine ("leaky gut" phenomenon) and sufficiently contributes to development of obesity and associated diabetes as well as of lipedema.[2] In females, such translocation occurs recurrently during the T4 sub-phase of the menstrual cycle before the onset of menses, which means that menstrual cycle affects not just endometrium but also the gut permeability.[29] Gut permeability also increases during the menopause.[30] Moreover, this "leaky gut" phenomenon is less pronounced in eumenorrheic women than in women taking oral contraceptive pills.[31] These new insights can substantially influence the treatment strategy for cellulite in the future since the management of endotoxemia can make the treatment outcomes more long-lasting.

This study has several limitations. First, this was a retrospective case-series study which did not allow any analysis of additional parameters such as demographic data or influence of UCTD. Second, the presented cohort of patients demonstrated a high variability of follow-up times ranged between 3 to 18 months (8.35 ± 4.44 months), which did not allow to make a precise and statistically supported conclusion about the characteristic decay times of treatment outcomes. Third, a relatively small sample size and retrospective type of the study did not allow a reliable statistical evaluation to answer the question how the number of treatment sessions influence the treatment outcomes and their stability. Additional studies will be needed to address these open question.

Conclusion

This clinical study demonstrated that application of TF-LDM waves of 1/3/10 MHz and 3/10/19 MHz produces a sufficient improvement in the cellulite skin, which is mainly caused by significant reinforcement of the dermis and skin-associated adipose tissue that connects the dermis with the superficial fascia. This modification has a long-term character and demonstrates progressive development that continues for at least over 6 months after cessation of treatment. This treatment method was highly accepted by participants who reported not only a high satisfaction with the treatment results, but also an improvement in their psychosocial state.

Ethics Statement

The present study was designed and conducted in accordance with ethical principles of the Declaration of Helsinki. The research was examined and permitted by the Ethics Review Board of the North-West Public Health Research Center (protocol 2021/43.1 of 14.12.2021).

Informed-Consent Statement

All patients who participated in this study signed a written informed consent allowing to publish their data and images for scientific purposes.

Disclosure

I.K. was the managing partner of the Wellcomet GmbH. He was not involved in clinical treatment or assessment of the treatment results. Wellcomet GmbH provided support in the form of salaries for I.K. but did not have any additional role in the decision to publish or the preparation of this manuscript. The commercial affiliation of I.K. with Wellcomet GmbH did not alter the adherence to all journal policies on sharing data and materials. The other authors have no conflicts of interest to declare.

References

1. Kruglikov IL, Scherer PE. Pathophysiology of cellulite: possible involvement of selective endotoxemia. *Obesity Rev*. 2023;24(1):e13517. doi:10.1111/obr.13517
2. Kruglikov IL, Scherer PE. Is the endotoxin–complement cascade the major driver in lipedema? *Trends Endocrinol Metab*. 2024;35(9):769–780. doi:10.1016/j.tem.2024.04.004
3. Zhang Z, Shao M, Hepler C, et al. Dermal adipose tissue has high plasticity and undergoes reversible dedifferentiation in mice. *J Clin Invest*. 2019;129:5327–5342. doi:10.1172/JCI130239
4. Kasza I, Kühn JP, Völzke H, et al. Contrasting recruitment of skin-associated adipose depots during cold challenge of mouse and human. *J Physiol*. 2022;600(4):847–868. doi:10.1113/JP280922
5. Kruglikov IL, Scherer PE. Dermal adipocytes: from irrelevance to metabolic targets? *Trends Endocrinol Metab*. 2016;27(1):1–10. doi:10.1016/j.tem.2015.11.002
6. Kruglikov IL, Zhang Z, Scherer PE. The role of immature and mature adipocytes in hair cycling. *Trends Endocrinol Metab*. 2019;30(2):93–105. doi:10.1016/j.tem.2018.11.004
7. Chen SX, Zhang LJ, Gallo RL. Dermal white adipose tissue: a newly recognized layer of skin innate defense. *J Invest Dermatol*. 2019;139(5):1002–1009. doi:10.1016/j.jid.2018.12.031
8. Cancello R, Zulian A, Gentilini D, et al. Molecular and morphologic characterization of superficial-and deep-subcutaneous adipose tissue subdivisions in human obesity. *Obesity*. 2013;21(12):2562–2570. doi:10.1002/oby.20417
9. Querleux B, Cornillon C, Jolivet O, Bittoun J. Anatomy and physiology of subcutaneous adipose tissue by in vivo magnetic resonance imaging and spectroscopy: relationships with sex and presence of cellulite. *Skin Res Technol*. 2002;8:118–124. doi:10.1034/j.1600-0846.2002.00331.x
10. Kruglikov IL, Scherer PE. Skin aging as a mechanical phenomenon: the main weak links. *Nutr Healthy Aging*. 2018;4(4):291–307. doi:10.3233/NHA-170037

11. Huang X, Li B, Hong W, Cao YP, Feng XQ. Effects of tension–compression asymmetry on the surface wrinkling of film–substrate systems. *J Mech Phys Solids*. 2016;94:88–104. doi:10.1016/j.jmps.2016.04.014
12. Van Oosten AS, Vahabi M, Licup AJ, et al. Uncoupling shear and uniaxial elastic moduli of semiflexible biopolymer networks: compression-softening and stretch-stiffening. *Sci Rep*. 2016;6(1):19270. doi:10.1038/srep19270
13. Yoshida Y, Kajiya K, Kishimoto J, Detmar M. Quantitative histological analyses and transcriptional profiling reveal structural and molecular changes of the dermal extracellular matrix in cellulite. *J Dermatol Sci*. 2018;92(1):6–9. doi:10.1016/j.jdermsci.2018.06.010
14. Smalls LK, Lee CY, Whitestone J, et al. Quantitative model of cellulite: three-dimensional skin surface topography, biophysical characterization, and relationship to human perception. *Int J Cosmet Sci*. 2005;56(2):105–120.
15. Ezure T, Amano S, Matsuzaki K. Infiltration of subcutaneous adipose layer into the dermal layer with aging. *Skin Res Technol*. 2020;28(2):311–316. doi:10.1111/srt.13133
16. Ortonne JP, Zartarian M, Verschoore M, Queille-Roussel C, Duteil L. Cellulite and skin ageing: is there any interaction? *J Eur Acad Dermatol Venereol*. 2008;22(7):827–834. doi:10.1111/j.1468-3083.2007.02570.x
17. Kruglikov IL, Scherer PE. Caveolin-1 as a target in prevention and treatment of hypertrophic scarring. *NPJ Regen Med*. 2019;4(1):9. doi:10.1038/s41536-019-0071-x
18. Kruglikov IL, Scherer PE. Control of adipose tissue cellularity by the terminal complement cascade. *Nat Rev Endocrinol*. 2023;19(12):679–680. doi:10.1038/s41574-023-00900-w
19. Samandari M, Abrinia K, Mokhtari-Dizaji M, Tamayol A. Ultrasound induced strain cytoskeleton rearrangement: an experimental and simulation study. *J Biomech*. 2017;60:39–47. doi:10.1016/j.jbiomech.2017.06.003
20. Kruglikov IL. Sehr hochfrequenter Ultraschall. *Der Hautarzt*. 2015;66(11):829–833. doi:10.1007/s00105-015-3676-z
21. Lucassen GW, van der Sluys WLN, van Herk JJ, et al. The effectiveness of massage treatment on cellulite as monitored by ultrasound imaging. *Skin Res Technol*. 1997;3(3):154–160. doi:10.1111/j.1600-0846.1997.tb00180.x
22. Watson JM, Kang'ombe AR, Soares MO, et al. Use of weekly, low dose, high frequency ultrasound for hard to heal venous leg ulcers: the Venus III randomised controlled trial. *Br Med J*. 2011;342(342):d1092. doi:10.1136/bmj.d1092
23. Cohen JL, Sadick NS, Kirby MT, et al. Development and validation of the clinician reported and participant reported photonumeric scales to assess buttocks cellulite severity. *Dermatol Surg*. 2020;46(12):1628–1635. doi:10.1097/DSS.0000000000002756
24. Young VL, DiBernardo BE. Comparison of cellulite severity scales and imaging methods. *Aesth Surg J*. 2021;41(6):NP521–NP537. doi:10.1093/asj/sjaa226
25. Ahn TH, Lee JS, Kim SY, et al. Application of dual-frequency ultrasound for reduction of perilesional edema and ecchymosis after rhinoseptoplasty. *J Cosmet Dermatol*. 2024;23(3):830–838. doi:10.1111/jocd.16040
26. Chervinskaya IG, Gaidash NV, Kruglikov IL. A retrospective pragmatic two-center clinical study to evaluate the clinical outcome of triple-frequency ultrasound in the treatment of mild-to-severe acne vulgaris. *J Cosmet Dermatol*. 2024. doi:10.1111/jocd.16672
27. McLaughlin PJ, Bakall B, Choi J, et al. Lack of fibulin-3 causes early aging and herniation, but not macular degeneration in mice. *Human Mol Gen*. 2007;16(24):3059–3070. doi:10.1093/hmg/ddm264
28. Waleczek FJG, Sansonetti M, Xiao K, et al. Chemical and mechanical activation of resident cardiac macrophages in the living myocardial slice ex vivo model. *Basic Res Cardiol*. 2022;117(1):63. doi:10.1007/s00395-022-00971-2
29. Roomruangwong C, Carvalho AF, Geffard M, Maes M. The menstrual cycle may not be limited to the endometrium but also may impact gut permeability. *Acta Neuropsychiatr*. 2019;31(6):294–304. doi:10.1017/neu.2019.30
30. Shieh A, Epeldegui M, Karlamangla AS, Greendale GA. Gut permeability, inflammation, and bone density across the menopause transition. *JCI Insight*. 2020;5(2):e134092. doi:10.1172/jci.insight.134092
31. Flood TR, Kuennen MR, Blacker SD, et al. The effect of sex, menstrual cycle phase and oral contraceptive use on intestinal permeability and ex-vivo monocyte TNFα release following treatment with lipopolysaccharide and hyperthermia. *Cytokine*. 2022;158:155991. doi:10.1016/j.cyto.2022.155991